

# ForgeHLS: A Large-Scale, Open-Source Dataset for High-Level Synthesis

Zedong Peng<sup>1</sup>, Zeju Li<sup>2</sup>, Mingzhe Gao<sup>1</sup>, Qiang Xu<sup>2</sup>, Chen Zhang<sup>1</sup>, and Jieru Zhao<sup>1\*</sup>

<sup>1</sup>Shanghai Jiao Tong University, Shanghai, China

<sup>2</sup>The Chinese University of Hong Kong, Hong Kong S.A.R.

**Abstract**—High-Level Synthesis (HLS) plays a crucial role in modern hardware design by transforming high-level code into optimized hardware implementations. However, progress in applying machine learning (ML) to HLS optimization has been hindered by a shortage of sufficiently large and diverse datasets. To bridge this gap, we introduce ForgeHLS, a large-scale, open-source dataset explicitly designed for ML-driven HLS research. ForgeHLS comprises over 400,000 diverse designs generated from 536 kernels covering a broad range of application domains. Each kernel includes systematically automated pragma insertions (loop unrolling, pipelining, array partitioning), combined with extensive design space exploration using Bayesian optimization. Compared to existing datasets, ForgeHLS significantly enhances scale, diversity, and design coverage. We further define and evaluate representative downstream tasks, such as Quality of Result (QoR) prediction and automated pragma exploration, clearly demonstrating ForgeHLS’s utility for developing and improving ML-based HLS optimization methodologies.

**Index Terms**—High-Level Synthesis, dataset, Large Language Model.

## I. INTRODUCTION

High-Level Synthesis (HLS) is a key technology in modern hardware design, enabling the transformation of high-level code, such as C, C++, or SystemC, into optimized hardware implementations. HLS serves as a bridge between software and hardware design, offering designers the ability to automatically generate hardware descriptions, such as Verilog or VHDL, from high-level algorithmic specifications. This process significantly reduces the time and complexity traditionally required in hardware design, making it a pivotal tool for accelerating the development of custom hardware solutions. A critical aspect of HLS is the use of pragmas. Pragmas are directives that guide hardware optimizations without altering algorithmic code, influencing performance, resource utilization, and power consumption. There are two ways to insert pragmas: by manually adding directive files, and by inserting pragmas directly in the source code.

HLS research has focused on several key downstream tasks, including QoR (Quality of Result) prediction [1, 2, 3, 4], and DSE (Design Space Exploration) [5, 6]. QoR prediction aims to estimate the latency and resource utilization. DSE focuses on systematically exploring different HLS pragma configurations to identify optimal design points that balance performance, resource usage and power consumption. Both tasks rely on large and high-quality datasets to improve the efficiency and effectiveness of HLS tools. However, existing datasets for HLS [7, 8, 9, 10] have been limited in scope

and size, often restricted to a small set of applications or a narrow range of hardware configurations. This limitation hinders progress in these critical research domains.

To address these challenges, we introduce **ForgeHLS**, a large-scale, open-source dataset featuring 429,276 HLS designs generated from 536 diverse C++ kernels. ForgeHLS is 10 times larger than existing HLS datasets [8, 9] and spans a broad spectrum of algorithms across various domains.

**Diverse Algorithm Coverage.** ForgeHLS collects real-world HLS kernels from established benchmarks as well as official Xilinx collections, such as Vitis HLS examples [11]. We provide a comprehensive collection of all above high-quality benchmarks and have unified them into a consistent format. Moreover, we introduce synthetic code to enhance our dataset. We collect a diverse list of algorithms and generate corresponding HLS kernel implementations. We leverage GPT-4o to generate C++ implementations for each algorithm and perform cross-validation to ensure the quality of the synthetic code. This comprehensive collection approach has enabled ForgeHLS to reach 536 unique kernels, representing an order of magnitude increase over existing HLS datasets.

**Automated Pragma Insertion.** We developed an automated code analysis workflow that extracts key information from HLS code and explore the full design space by generating all possible combinations of pragma types and factors. For large-scale kernels that cannot be fully explored through exhaustive enumeration, we utilize Bayesian optimization to guide the design space exploration. In previous datasets, the combinations of pragmas are typically defined in a script or a separate file [8, 9, 10], requiring users to generate a large amount of feasible HLS designs for training and testing. This process incurs additional substantial effort and time cost. In contrast, we provide feasible HLS designs with corresponding post-HLS performance metrics, and directly insert pragmas into source code to make generated HLS designs easier to use. Our direct pragma insertion allows the code to be easily used for large language model (LLM) and other downstream tasks. This automated pragma insertion workflow will also be open-source, ensuring the dataset’s extensibility to support additional pragma types in the future. By incorporating a comprehensive set of pragmas, we generate 429,276 HLS designs that capture both the functional and structural complexities of HLS code.

**Multi-task Evaluation.** After constructing our comprehensive dataset, a series of HLS downstream tasks can be

investigated and conducted. Specifically, we present two representative tasks: HLS QoR (Quality of results) prediction and HLS pragma DSE. These tasks not only showcase the effectiveness of ForgeHLS but also serve as practical examples for reference in other HLS optimization tasks.

In summary, our contributions offer a valuable foundation for the EDA community, promoting advancements in model performance and accelerating machine learning-driven innovation in HLS. The main contributions are:

- 1) We propose a large-scale, diverse HLS dataset that covers a broad spectrum of algorithms and application domains.
- 2) We propose an automated workflow for pragma insertion, extensively embedding HLS pragmas into our C++ kernel code.
- 3) We define two representative downstream tasks to evaluate our dataset.

## II. RELATED WORK

### A. HLS Datasets

Numerous efforts have been made to develop datasets and frameworks for HLS research, as listed in Table I and Table II. DB4HLS [7] provided a database of over 100,000 HLS design points collected from MachSuite through exhaustive design space exploration. HLSyn [10] offers 42,000 labeled designs from MachSuite and PolyBench. HLSDataset [9] and HLSFactory [8] extended their datasets on more benchmarks. However, only a subset of their kernels has been open-sourced or includes HLS pragma annotations, and access to some of the post-HLS features is limited or unavailable. Moreover, there are relatively small-scale HLS benchmarks that are commonly favored in mainstream training. These include PolyBench [12], CHStone [13], MachSuite [14], and Rosetta [15]. These benchmarks provide kernel source code, and many datasets are derived from these kernels through DSE to construct their datasets.

Current HLS datasets have several key limitations that hinder their effectiveness for machine learning model training. First, their sources are limited, with most datasets coming from benchmark suites. Second, these datasets lack standardization in format, making it difficult to apply and compare the code uniformly across different sources. Third, they often lack essential post-HLS files, such as ADB (Architecture Description Block) files, which are necessary for CDFGs (constructing control-data flow graphs). Table I compares different methods in multiple dimensions.

### B. HLS Downstream Tasks

HLS research has introduced several downstream tasks, such as *QoR (quality of results) prediction* and *DSE (design space exploration)* of HLS pragmas. In the *QoR prediction* task, prior research leverages machine learning to estimate the performance and area for HLS designs early in the design cycle. These methods enable faster and more efficient optimization without running the time-consuming synthesis

TABLE I: Comparison between mainstream datasets. “Code with Pragma” indicates whether the source code of HLS designs inserted with pragmas is provided or not; “Graph”: files used to generate graph; ✓: fully supported; ●: partially supported, partially open-source, or requiring additional effort to access; ✗: not supported

Feature	DB4HLS [7]	HLSyn [10]	HLSDataset [9]	HLSFactory [8]	ForgeHLS
<b>Source</b>					
CHStone	✗	✗	●	●	✓
MachSuite	✓	✓	✓	✓	✓
Polybench	✗	✓	●	●	✓
Rosetta	✗	✗	✓	✓	✓
Vitis-Examples	✗	✗	●	●	✓
Synthetic Code	✗	✗	✗	✗	✓
<b>Pre-HLS</b>					
Code with Pragma	✓	●	✗	✗	✓
<b>Post-HLS</b>					
Latency	✓	✓	✗	●	✓
Resources	✓	✓	●	●	✓
Graph	✗	✓	✗	●	✓

flow. Different ML techniques, such as gradient-boosted machine (GBM) [16], XGBoost [17], graph neural networks (GNNs) [1, 2, 18], have been explored to predict post-HLS or post-route QoR at the source code level or the intermediate representation (IR) level. However, their models are trained on small-scale datasets constructed with typical HLS benchmarks, which limits their ability to generalize to new designs with unseen code structures.

In the task of DSE of HLS pragmas, various configurations of HLS pragmas are evaluated and compared to find optimal design parameters with best QoR. Different DSE frameworks are proposed to improve search quality and efficiency, utilizing heuristics [19], conventional methods such as genetic algorithms or simulated annealing [20, 21], or ML-based search [1, 16, 18, 22]. Moreover, recent advancements further support automatic pragma insertion after the completion of DSE [23, 24]. Efficient and high-quality DSE reduces the manual effort required for tuning and optimizing HLS code, reducing the development time. However, these frameworks are often built and evaluated using typical HLS benchmarks like PolyBench, which makes it difficult to assess their effectiveness on more complex designs.

## III. DATASET

### A. Dataset Overview

As shown in Table II, ForgeHLS is composed of real-world code from established HLS benchmarks [11, 12, 13, 14, 15], along with synthetic code generated from a variety of algorithms [25, 26]. The kernels represent the C++ source code without pragma, while the designs capture the kernel variations created by embedding different types and factors of HLS pragmas. On average, each kernel in ForgeHLS have 800.9 designs, 9.4 pragmas, and 394.4 tokens in average, indicating the complex code structures and diverse pragma design space within the dataset. An overview of the dataset construction workflow is presented in Figure 1.

Specifically, the data construction flow involves two key stages: collection and generation of kernels (Sec. III-B) and design space exploration for pragma insertion (Sec. III-C).

TABLE II: Statistics of the ForgeHLS dataset.

Source	#K	#D	A#D	A#P	A#T
<b>Real-World Code</b>					
CHStone [13]	4	4,684	1171	24.0	5932.7
MachSuite [14]	19	16,803	884.4	18.9	990.8
PolyBench [12]	26	22,897	880.7	18.6	486.2
Rosetta [15]	5	1,849	369.8	197.8	8985.8
Vitis-Examples [11]	41	22,794	556.0	8.2	673.8
<b>Synthetic Code</b>					
HLS algorithms	113	93,379	826.4	8.5	285.6
Leetcode algorithms	22	18,780	853.6	5.6	203.2
Operators	154	85,099	552.6	5.5	165.7
RTL chip [25]	16	12,922	807.6	6.9	199.8
RTL ip [25]	5	4,874	974.8	5.6	279.5
RTL module [25]	131	145,195	1108.4	5.2	128.2
<b>Ours in Summary</b>	<b>536</b>	<b>429,276</b>	<b>800.9</b>	<b>9.4</b>	<b>394.4</b>
<b>Related Work</b>					
DB4HLS	19	124,106	6531.8	6.5*	2270.7*
HLSyn	42	42,000	1000.0	7.6	629.9
HLSDataset	34	18,876	555.1	-	-
HLSFactory	82	-	-	-	-

#K: number of kernels; #D: total number of designs; A#D: average number of designs per kernel; A#P: average number of pragmas per kernel; A#T: average number of tokens per kernel; -: unavailable or not reported; \*: data calculated by us.

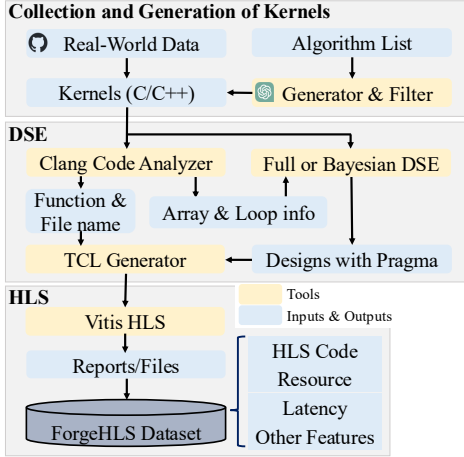


Fig. 1: The overview workflow of our dataset construction.

Based on this flow, we can construct a dataset that is both comprehensive and versatile, suitable for multiple HLS-related downstream tasks (Sec. IV).

### B. Collection and Generation of Kernels

We adopt a dual approach: aggregating real-world HLS kernels from open-source repositories and generating diverse algorithmic implementations through GPT-4o to collect rich kernels. For real-world HLS code, we aggregate data from a variety of established benchmarks to ensure broad coverage and applicability. These sources include: PolyBench [12], MachSuite [14], CHStone [13], and Rosetta [15]. Additionally, we include a significant collection from Vitis HLS official codebase [11].

For generated C++ code by GPT-4o, we provide a cross-verification workflow to ensure correctness, as shown in Fig. 2. We prioritize the inclusion of a wide range of HLS-compatible

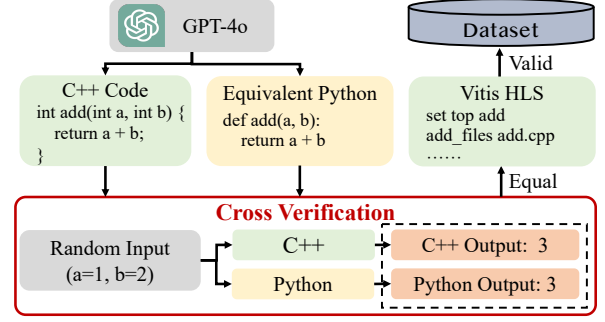


Fig. 2: The structure of generator and filter.

algorithms. ForgeHLS covers various algorithms: 1) *fundamental operators*, such as adders, counters, and dividers, which are critical for low-level hardware designs; 2) *typical HLS computation-intensive algorithms*, such as matrix multiplication, FFT, signal processing algorithms, I2C master/slave controllers, and IP checksum calculation, that are feasible for hardware implementation and commonly optimized in HLS. This category also includes commonly used kernels from deep learning, such as LSTM cells and DNN layers; 3) *Leetcode algorithms*, including representative C/C++ algorithms such as binary search and merge sort, solving classical algorithmic problems that are often used for algorithmic training and benchmarking; 4) *RTL (Register-Transfer Level) designs implemented in HLS C code*, including RTL chips, RTL IPs and RTL modules, following the same description and specification as those of the RTL dataset [25].

We input the specifications for the algorithm description and HLS code rules into GPT-4o, which then automatically generate the corresponding code without HLS pragmas. The HLS code rules ensure correct input and output parameter usage, maintain scalability for future pragma additions, enforce strict compliance with the C++11 standard, and prohibit the use of unsupported C/C++ constructs. The unsupported C/C++ constructs include system calls, dynamic memory usage, pointer limitations, recursive functions, undefined behaviors, and virtual functions and pointers. We run a single-pass HLS flow to validate the syntactic accuracy of LLM generated code. To validate the functional accuracy, we employ a cross-verification approach leveraging GPT-4o as an assistant. Specifically, we provided GPT-4o with an algorithm description and the corresponding implementation, requesting it to generate a Python version of the same algorithm. This Python implementation served as a reference model for validation. Only when the synthetic code meets both syntactic and functional correctness criteria, we collect it in our ForgeHLS. After that, we apply DSE on kernels to further enhance our dataset.

### C. Design Space Exploration for Pragma Insertion

After collecting both real-world and synthetic HLS data, we perform full Design Space Exploration (DSE) and Bayesian DSE to systematically expand the design space coverage.

For full DSE, we propose a pragma insertion workflow, as shown in Fig. 3. The process begins with Clang, which performs a syntactic analysis of the C++ source code to extract essential information needed for DSE. This includes

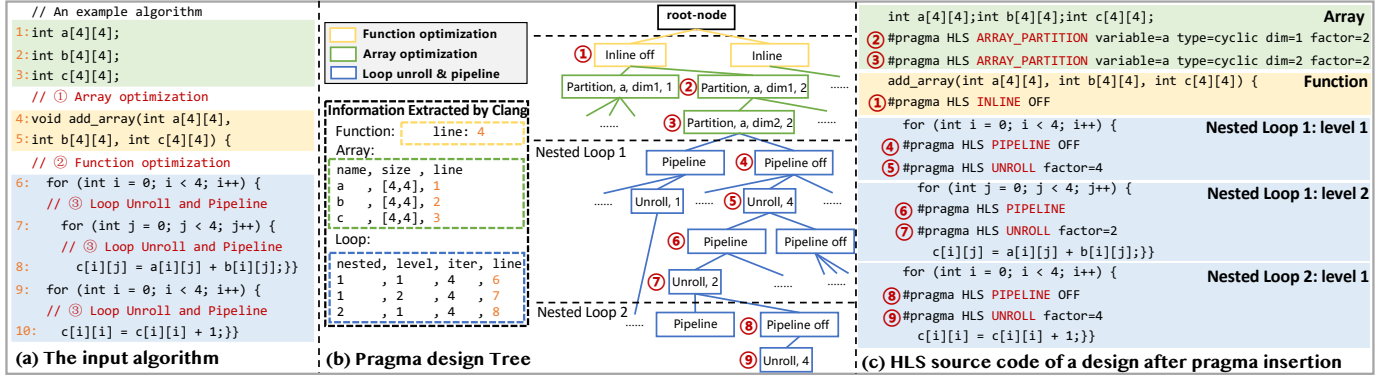


Fig. 3: The process of full design space exploration: (a) showcases an input algorithm written in C++ with a nested loop structure and array manipulations; (b) illustrates the pragma design tree, detailing the hierarchical insertion with multiple optimization options; and (c) demonstrates an example of HLS code after pragma insertion, where multiple pragmas are automatically annotated into the source code, enabling diverse HLS design generation.

### Algorithm 1: Bayesian DSE Explorer

**Input:** A C/C++ kernel  $\mathcal{K}$

**Output:** A diverse set of designs  $\mathcal{D}$  with pragmas

```

1 pragma_cfg ← GetCodeInfo( $\mathcal{K}$ )
2  $\mathcal{D} \leftarrow \emptyset$ 
3 for  $i = 1$  to  $N_{opt}$  do
4   pragma_cfg.update ←
     nRandomStarts( $\mathcal{K}$ , pragma_cfg, random)
5    $\mathcal{D} \leftarrow \mathcal{D} \cup$  nRandomStarts
6   for  $j = 1$  to  $N_{calls}$  do
7     DesignPoint ← Generate( $\mathcal{K}$ , pragma_cfg)
8     resource, latency ← RunHLS(DesignPoint)
9      $\mathcal{D} \leftarrow \mathcal{D} \cup$  DesignPoint
10    cost ← CalculateCost(resource, latency)
11    pragma_cfg.update ←
       Bayesian(cost, pragma_cfg)
12 return  $\mathcal{D}$ 

```

loop trip counts, loop locations, array sizes and dimensions, array definition locations, and the identification and location of the top function. Such analysis ensures that the appropriate pragmas can be inserted accurately into the code.

Following this, we construct a pragma insertion tree to guide the selection of pragma factors. Specifically, we determine whether to enable or disable function inlining and pipelining on the first line inside each function. For the array partition pragma, we choose the target array, the dimension to apply, the partition factor, and the partition type. For loop optimizations, we decide whether to apply loop pipeline, whether to apply unroll, and if unrolling is applied, what unroll factor to choose.

It is worth emphasizing that the full DSE does not exhaustively enumerate all pragma permutations. Instead, it follows a set of essential HLS design principles: **1)** if the outer loop of a nested loop structure is pipelined, the inner loop will not use the unroll pragma; **2)** unroll and partition factor selection is restricted to powers of 2 within the range of the upper limit

of the loop trip count or array size; **3)** if the current branch of the pragma design tree becomes excessively large, pruning is performed to retain only the designs whose unroll and partition factors are equivalent. By applying these rules, we eliminate invalid pragma combinations, which helps in reducing the dataset size without compromising its quality. A traversal in design tree from the root node to a leaf node represents one pragma configuration. Each path encodes a sequence of pragma decisions, and the resulting leaf node corresponds to a unique design instance. This tree-based representation enables systematic exploration of the design space, where constraints can be enforced dynamically during traversal to avoid infeasible or redundant configurations.

However, due to the combinatorial nature of pragma factor selection, the number of design instances in full DSE grows exponentially with the number of applied pragmas. For complex kernels with more than 10 pragmas, full design space traversal can easily yield millions of design candidates. Performing HLS synthesis on such a large number of configurations is computationally prohibitive and contradicts the core objective of our dataset—efficiently generating high-quality, diverse design instances.

To address this challenge, we propose a Bayesian DSE strategy tailored for complex design cases. Instead of exhaustively evaluating the entire design space, Bayesian DSE leverages a probabilistic surrogate model to iteratively select promising configurations based on previous evaluation results. Algorithm 1 presents our design space exploration strategy based on Bayesian optimization. As a lightweight and flexible exploration technique, it aims to efficiently discover diverse high-quality design candidates without exhaustively enumerating the entire pragma space. Given a C/C++ kernel  $\mathcal{K}$ , we first extract its pragma configuration space using Clang static analysis (line 1). The algorithm begins by seeding the design set  $\mathcal{D}$  with a set of randomly sampled initial designs (lines 3 to 5), which serve as starting points for exploration. Then, for each optimization round, the algorithm iteratively performs Bayesian optimization over  $N_{calls}$  steps (lines 6 to 11). At each

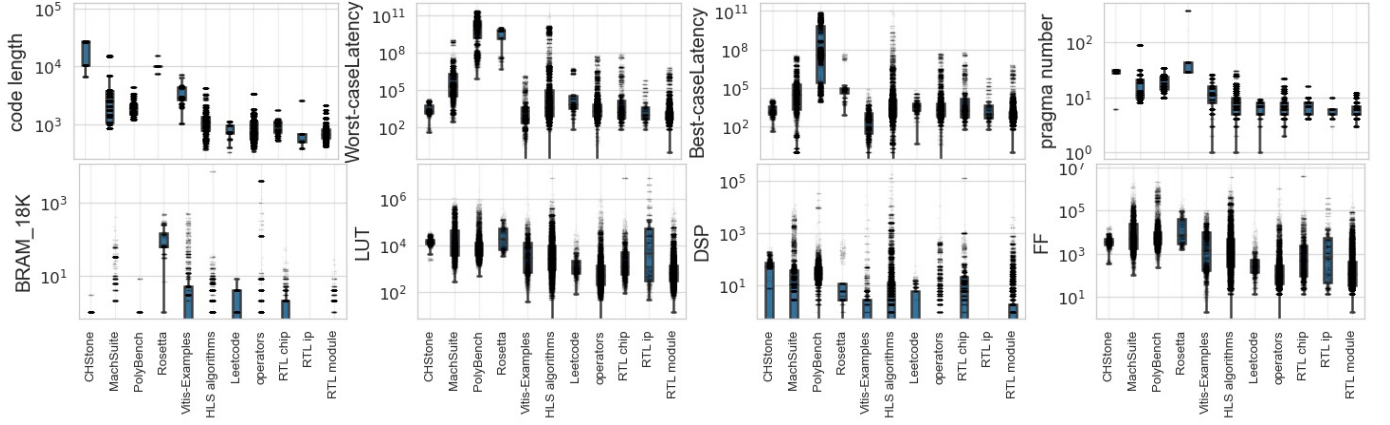


Fig. 4: Detailed distribution of ForgeHLS across data source. Each dot represents one individual design.

iteration, it generates a new design with pragma *DesignPoint* from the current pragma configuration (line 7), evaluates the design using HLS synthesis (line 8), and collects resource and latency information. Each *DesignPoint* is stored in  $\mathcal{D}$  (line 9). Based on the observed quality metrics, a cost is calculated (line 10) to reflect the overall design objective. Finally, the Bayesian optimizer updates its surrogate model and acquisition function based on the new observation, and selects the next pragma configuration accordingly. The algorithm continues until the optimization round completes.

This iterative process allows the exploration to focus on promising regions of the design space while maintaining diversity through random initialization. The accumulated design set  $\mathcal{D}$ , containing pragmas and QoR results, is returned for constructing the ForgeHLS dataset. Notably, our goal with DSE is to expand design space coverage rather than solely focus on identifying a Pareto curve. For downstream tasks such as QoR prediction, the value of non-Pareto-optimal designs in ForgeHLS lies in the trade-offs they represent, which provide valuable insights. Our code analysis extracts all relevant details about arrays and loops, and we randomly configure all the pragmas, running HLS to sample non-Pareto-optimal designs. These random starting points also serve as a source of data. After collecting all designs for a given kernel, we label the generated pareto points as Pareto within our dataset. Although these points may slightly deviate from ground-truth pareto-optimal designs as exhaustive evaluation of the entire design space is computationally infeasible, it is acceptable to use these near-optimal designs for model training and development. Users can also adopt their customized DSE algorithms to generate other near-optimal points. A more detailed analysis of the design space coverage in ForgeHLS will be provided in Sec. IV-A.

#### IV. EVALUATION

We utilize Vitis HLS 2023.2 to collect ground-truth latency and resource usage as our dataset labels. The clock is set to 10 ns and the target FPGA is xcu280-fsvh2892-2L-e.

##### A. Design Space Coverage

In this section, we evaluate the effectiveness of our approach in expanding the design space coverage, particularly with

respect to latency and resource usage, which are essential metrics for model training in downstream tasks such as QoR prediction. For latency, we use the Worst Case Latency extracted from the Vitis HLS report, and for resource usage, we compute the Average Resource Usage (ARU) across four key resource (BRAM, FF, LUT, and DSP). The ARU is calculated using the following equation 1.  $N$  represents the number of resources for which  $\text{Available Resource}_k \neq 0$ .

$$\text{ARU} = \frac{1}{N} \sum_{k \in \text{BRAM, FF, LUT, DSP}} \frac{\text{Used Resource}_k}{\text{Available Resource}_k} \quad (1)$$

**Progressive Dataset Expansion.** We have progressively expanded our dataset to achieve broader kernel coverage. Initially, we used standard HLS benchmark suites, such as CHStone, MachSuite, PolyBench, and Rosetta. We then extended the dataset by incorporating kernels from the Vitis Examples industry database, which significantly improved coverage. Furthermore, the inclusion of kernels generated by LLM Synthetic Code contributed to another substantial increase in design space coverage. As shown in Fig. 5, these kernels, sourced from diverse origins, complement each other in expanding the design space and enriching dataset diversity.

**Detailed Distribution of ForgeHLS.** The detailed distribution of the dataset across different sources is shown in Fig. 4. We present key metrics of our dataset, including the code length, latency, number of pragmas and resource usage. Each data point in these plots represents an individual design, demonstrating the spread of design characteristics across sources. This analysis shows the incremental improvement in coverage as new sources are added, particularly highlighting how LLM-generated synthetic code helps fill gaps in kernel diversity and design complexity. From this distribution, it can be observed that the synthetic code exhibits a relatively rich distribution overall. While the number of pragmas and tokens in synthetic code is slightly lower compared to real-world benchmarks, the feature distribution in terms of resource usage and latency appears comparable. This indicates that its diversity in resource and latency characteristics is sufficient for robust model training.

**Comparison with Existing Datasets.** While we compare our dataset to HLSyn and DB4HLS in Fig. 5, it is important to



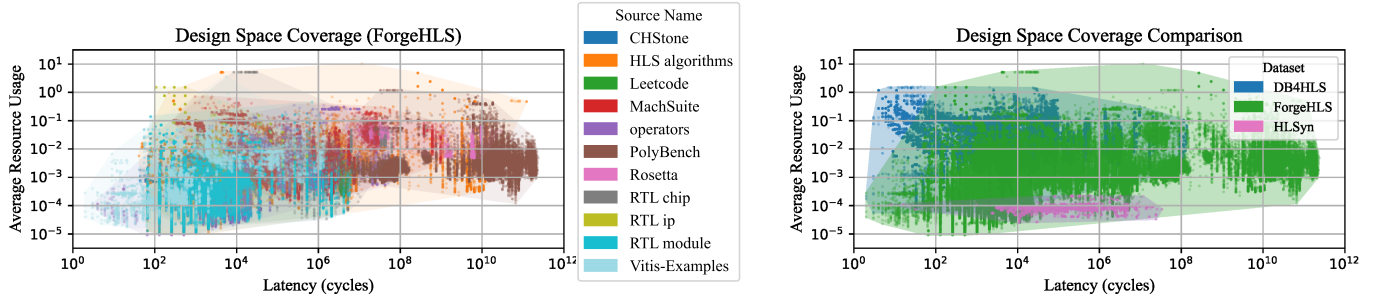


Fig. 5: Design space coverage across different dataset.

note that we have not included comparisons with HLSDataset and HLSFactory. This omission is due to the incomplete accessibility of latency and resource data from these sources. Both HLSDataset and HLSFactory have only released a limited portion of their latency and resource metrics.

It is also worth noting that HLSyn’s design leverages AutoDSE [5], resulting in designs that tend to exhibit low resource usage. This leads to a lack of diversity in design solutions. For robust model training, it is crucial to consider not only Pareto-optimal solutions but also non-Pareto solutions. These non-Pareto solutions can also provide valuable insights into the trade-offs between resource usage and latency, contributing to the robustness of the model and its ability to generalize to a broader range of design scenarios.

Despite this limitation, as shown in Fig. 5, our dataset demonstrates superior coverage in terms of both latency and resource usage compared to HLSyn and DB4HLS. Our dataset’s larger scale and more comprehensive distribution make it better suited for addressing the diverse challenges encountered in real-world applications. This broader coverage enhances the robustness of model training for tasks like QoR prediction and hardware design optimization.

In conclusion, the expanded coverage of latency and resource usage in our dataset strengthens its ability to model a wider range of hardware designs, which is crucial for advancing QoR prediction and other downstream tasks in hardware design optimization.

### B. Downstream Task 1: HLS QoR Prediction

In this downstream task, we train GNN models and LLMs on various datasets for post-HLS QoR prediction. Specifically, we aim to explore two key questions: **1)** can GNNs accurately predict the true QoR values in a dataset as large as ours? **2)** can LLMs predict the corresponding QoR metrics after fine-tuning, and how accurate are their predictions?

To fairly compare the model’s generalization ability, we propose the **Unseen Test Set**, which is constructed by selecting 10% of kernels from ForgeHLS, resulting in a set of 57 kernels, each with its corresponding designs. By doing so, we ensure that all training sets do not include any kernels from the Unseen Test Set, allowing us to evaluate the model with on a consistent metrics. We also build **Standard Test Set** for each dataset. The Standard Test Set is created by performing a 90:10 split from each dataset designs, representing the model’s fitting ability. For the GNN training baseline from [2], this

TABLE III: Downstream Task 1. Performance comparison of GNNs and LLMs for QoR prediction. **#[2]**: the dataset without pragmas used for GNN training in [2]; **#P-ForgeHLS**: dataset with pragmas, derived from the PolyBench portion of ForgeHLS.

MAPE (%)	Standard Test Set			Unseen Test Set		
	DSP	FF	LUT	DSP	FF	LUT
<b>Model-Trainset</b>						
RGCN- <b>#[2]</b>	18.8	26.5	32.4	> 5000	2191.7	1004.0
RGCN- <b>#P-ForgeHLS</b>	47.4	25.4	21.8	251.7	1521.4	174.1
RGCN-ForgeHLS	84.7	228.4	44.1	123.1	511.7	62.5
SAGE- <b>#[2]</b>	<b>17.0</b>	<b>20.8</b>	18.7	136.2	818.2	103.5
SAGE- <b>#P-ForgeHLS</b>	52.8	26.1	<b>12.7</b>	219.0	2026.2	384.9
SAGE-ForgeHLS	87.1	101.6	34.3	94.1	1833.4	68.8
LLaMA3-7B-Origin	140.9	2448.5	217.1	142.9	2428.6	221.3
LLaMA3-7B-DB4HLS	72.4	901.7	602.4	70.2	3529.3	1529.5
LLaMA3-7B-ForgeHLS	23.1	61.7	26.0	<b>55.1</b>	111.2	59.7
Qwen-7B-Origin	1990.8	2250.6	309.8	2644.4	3791.5	413.7
Qwen-7B-DB4HLS	81.1	481.0	394.8	73.2	2665.7	951.6
Qwen-7B-ForgeHLS	46.6	49.3	27.0	84.3	96.1	65.0
Mis-7B-Origin	> 5000	287.5	338.4	> 5000	209.8	70.6
Mis-7B-DB4HLS	> 5000	3369.1	2933.7	> 5000	3780.8	3656.4
Mis-7B-ForgeHLS	51.8	54.5	22.9	58.6	<b>73.3</b>	<b>37.1</b>

involves replicating the original methodology by training on the provided training set and evaluating the model using the corresponding test set. For GNN training on ForgeHLS and all LLMs training, the Standard Test Set is created by splitting the designs in a 90:10 ratio from the respective training sets. Unlike the Unseen Test Set, the Standard Test Set may contain kernels that overlap with those seen during training. It is important to note that the training set used for the Standard Test Set in ForgeHLS is the remaining kernel portion of the dataset not included in the Unseen Test Set. Therefore, the Unseen Test Set does not have any bias towards ForgeHLS.

We follow the knowledge rich approach from [2] for GNN training, where ADB files are compiled into control data flow graphs to serve as input. Each GNN is set as 5 layers with a hidden-dimension size of 300, and 300 epochs for Adam optimizer. For LLMs, we train mainstream open-source models by LoRA [27] fine-tuning the LLMs, with Code-QoR pairs as input in the format {"input": "code with HLS pragma", "output": {"lut": lut\_num, "dsp": dsp\_num, ...}}. This setup enables the LLMs to directly predict QoR metrics. The key LoRA training settings are as follows: the LoRA rank is set to 32, and the LoRA alpha is set to 64. We use MAPE (Mean Absolute Percentage Error) as the metric to evaluate

prediction errors. In the evaluation of QoR, we focus on LUT, DSP, and FF as the primary resource metrics. BRAM resources were not included in the evaluation because our experiments primarily target designs that do not rely heavily on large memory blocks. Many of the kernels in our dataset are computationally intensive and do not require significant amounts of block RAM, which makes LUT, DSP, and FF more relevant for the analysis.

We only compare our ForgeHLS with the previous DB4HLS dataset because both ForgeHLS and DB4HLS contain code with directly inserted pragmas, making them suitable for LLM training. In contrast, other datasets typically define pragmas in separate scripts or files, which results in a multi-file structure that complicates usage and is less suitable for efficient LLM training. Additionally, none of the previous datasets provide the ADB graph files required by [2], so we choose to compare our dataset with both the dataset from [2] and the PolyBench portion of ForgeHLS for comparison. Table III exhibits the performance of QoR predictions on GNNs and LLMs.

**GNN Performance in the Standard Test.** For the Standard Test, the MAPE on #[2] is lower than on ForgeHLS, which can be attributed to two main factors. First, the training and test sets in #[2] lack pragma insertion and consist of only 18,600 kernels, compared to the 429,276 designs in ForgeHLS with diverse pragma variations. The limited diversity in #[2] enables the GNN trained on this dataset to perform better on the standard test set, while the GNN trained on ForgeHLS struggles due to the larger and more complex dataset. Second, to ensure a fair comparison, we trained the GNN model on ForgeHLS with the same configuration, including graph layers, graph dimensions and training epochs. This configuration may have allowed the GNN to capture most of the knowledge from the simpler #[2] dataset, but for the more complex ForgeHLS, larger graph dimensions and more training epochs may improve performance on the standard test set. These results highlight the increased complexity and richness of the code patterns in our dataset, as well as the limitations of GNNs when applied to large, complex datasets. The answer to the first question is that GNNs, while effective in certain scenarios, lack the precision to consistently predict true QoR values for a dataset as extensive as ours. Thus, this leads to the second LLMs direct prediction question.

**Generalization Ability: GNN vs. LLM.** We evaluate the generalization ability of different trained models on the fair Unseen Test, where LLMs generally show superior performance. This can be attributed to two key factors. First, in terms of the number of learnable parameters, the GNN model in our configuration has approximately 450,000 parameters, while the LoRA fine-tuned LLMs involve over 1,000,000 learnable parameters. This significant difference in capacity indicates that LLMs have a greater ability to capture complex patterns, which is beneficial for accurate QoR prediction on the challenging Unseen Test. Second, LLMs are pretrained on vast amounts of diverse data, which enhances their generalization ability. This extensive pretraining allows LLMs to better handle unseen kernel structure, including analyzing diverse HLS

code encountered in the Unseen Test, or capturing pragma information and influence effectively.

**Standard vs. Unseen Test.** From the results across different datasets, we observe that models generally perform better on the Standard Test Set, as expected, due to its in-distribution nature, meanwhile the Unseen Test Set is more challenging. The Standard Test Set represents the model’s in-distribution fitting ability, where the training and test sets may contain overlapping kernels. In contrast, the Unseen Test Set consists of kernels that are entirely excluded from the training process, providing a stricter evaluation of generalization. The performance drop on the Unseen Test Set emphasizes the challenges of generalizing to new, unseen kernels, especially for GNN models. In contrast, LLMs consistently demonstrate better performance on the Unseen Test Set, indicating their superior ability to generalize across diverse HLS code patterns. This advantage is likely due to their large-scale pretraining and their capacity to capture complex relationships in data.

The QoR prediction task underscores the potential of LLMs in accurately predicting HLS performance, while also presenting new challenges for training GNN prediction models on large-scale datasets.

### C. Downstream Task 2: Automatic HLS Pragmas Exploration

From the first downstream task, we can infer that LLMs possess a certain level of HLS capability. Considering pragmas, which are a crucial aspect of HLS code, evaluating the performance of LLMs in handling and optimizing pragmas becomes essential. Using existing LLMs to insert pragmas into HLS code presents several challenges: incorrect pragma insertion locations, lack understanding of hardware-specific characteristics, resulting in synthesis failure, and provide sub-optimal pragma choices.

Our dataset has a large number of C++ kernels without pragma, and corresponding designs with pragma. It is not difficult to envision the potential for utilizing our HLS data to training an automatic pragma inserter based on LLM. Out of 536 ForgeHLS kernels, we use 90% kernels as the training set and reserve the remaining 10% as the test set. We define Pareto designs within our dataset as the dominant solutions in the trade-off between latency and ARU, where no design can improve one of the metrics without sacrificing the other. Then we divide the designs on Pareto curve into three categories: high, medium, and low resource usage. The top one-third of the points in terms of ARU are classified as high resource usage, the middle one-third as medium, and the remaining one-third as low. Lastly, we construct Kernel-Design pairs in the format {"instruction": "optimize for low resource usage and high latency.", "input": origin code, "output": Pareto design code with HLS pragma consuming low resource usage and high latency"}. By doing so, our trained pragma inserter can generate Pareto-optimal pragma designs for varying resource usage scenarios based on the input kernel code.

We fine-tune the LLaMA3, Qwen, and Mistral models using the LoRA[27] method and evaluate their performance on a subset of 10% kernels from ForgeHLS. For each design generated based on the model’s pragma suggestions, we run the HLS flow and measure the synthesis pass rate. The results, shown in Table IV, indicates that fine-tuning the LLMs on our dataset leads to higher synthesis pass rates for the generated HLS code with inserted pragmas. To further assess the quality of the generated pragma designs, we compare the predicted Pareto designs under three strategies with the ground-truth Pareto designs provided in our dataset. We use the Adjusted Distance to Reference Set (ADRS) as the evaluation metric. A lower ADRS value indicates that the generated designs are closer to the true Pareto front. The ADRS is computed as:

$$\text{Average ADRS} = \frac{1}{N} \sum_{k=1}^N \frac{1}{|\Gamma_k|} \sum_{\gamma \in \Gamma_k} \min_{\omega \in \Omega_k} \delta(\gamma, \omega) \quad (2)$$

$$\delta(\gamma, \omega) = \max \left\{ 0, \frac{l(\gamma) - l(\omega)}{l(\omega)}, \frac{r(\gamma) - r(\omega)}{r(\omega)} \right\} \times 100\%. \quad (3)$$

where  $N$  denotes the total kernel number,  $k$  denotes the kernel index,  $\Gamma_k$  denotes the exact Pareto-optimal set of kernel  $k$  in ForgeHLS, and  $\Omega_k$  represents the fine-tuned model predicted Pareto-optimal set in different resource usage strategy for kernel  $k$ . The term  $\delta(\gamma, \omega)$  calculates the normalized distance between two design points.  $l(\cdot)$  refers to the cycle latency of design point, extracted from the report generated by HLS. And  $r(\cdot)$  refers to ARU of the design point, calculated in equation 1. The expression  $\max \{0\}$  in  $\delta(\gamma, \omega)$  ensures that if the proposed method generates a better pragma combination than the ground truth within our dataset, it will be considered to have a zero distance to Pareto curve, which is not penalized. As shown in Table IV, the results demonstrate the effectiveness of fine-tuning LLMs on our dataset for automatic HLS pragma insertion.

**Increased HLS Pass Rate.** After training, the HLS pass rate increases significantly across all LLMs. For instance, the LLaMA3-7B model trained on ForgeHLS achieves a pass rate of 69%, compared to just 19% for the origin model. The improvement indicates that the trained LLMs are better at inserting valid pragmas. Specifically, model becomes more adept at avoiding invalid pragma insertion locations, improper pragma formats, configuration issues, and C++ syntax errors in the HLS code. This suggests that fine-tuning LLMs on our dataset improves LLMs’ understanding of HLS code format and syntax.

**Reduced ADRS.** The ADRS is significantly reduced after fine-tuning, indicates that the LLMs, after training, are more adept at generating pragma configurations that are closer to the true Pareto-optimal designs. This further emphasizes the potential of LLMs in DSE, where they can optimize HLS code for better resource usage and latency trade-offs.

**Performance on Full ForgeHLS.** Despite the improvements in HLS pass rates and ADRS reduction, the ADRS values remain relatively high when training on the full ForgeHLS dataset, compared to only training on synthetic part

TABLE IV: Downstream Task 2. Comparison of Pragma Exploration Performance Across Different LLMs trained on Two Datasets: **ForgeHLS** and **Synthetic Part of ForgeHLS**

Model	HLS Passed(%)	Average ADRS(%)
<b>Synthetic Part of ForgeHLS</b>		
LLaMA3-7B-Origin	77	131.62
LLaMA3-7B-Finetuned	94	1.64
Mistral-7B-Origin	8	40.00
Mistral-7B-Finetuned	<b>97</b>	<b>0.62</b>
<b>ForgeHLS</b>		
LLaMA3-7B-Origin	19	1554.32
LLaMA3-7B-Finetuned	<b>69</b>	48.68
Qwen-7B-Origin	27	1093.96
Qwen-7B-Finetuned	54	<b>38.36</b>
Mistral-7B-Origin	8	163.71
Mistral-7B-Finetuned	58	39.62

of ForgeHLS. This highlights the richness and quality of our ForgeHLS, which offers a broader range of HLS code patterns and kernel configurations compared to traditional datasets. The relatively larger ADRS when training on ForgeHLS suggests that more effective learning strategies are needed to fully exploit the diversity and complexity of our dataset. This calls for the development of more advanced models or training methods to leverage the full potential of our dataset for optimizing HLS designs.

## V. FUTURE WORK

Our future work will focus on expanding the ForgeHLS by adding more kernels and incorporating additional DSE. This will further diversify the dataset, enabling more robust models for predicting QoR metrics at scale. There is a clear need for more advanced models that can handle the complexity of such large datasets, and we call for the development of models with better generalization capabilities, such as enhanced GNNs or more powerful LLM architectures. Additionally, exploring new downstream tasks using our dataset, such as automated pragma optimization or hardware-specific design space exploration, will be crucial. Leveraging reinforcement learning or evolutionary algorithms for pragma insertion and resource allocation could help optimize performance further.

## VI. CONCLUSION

In this paper, we introduced **ForgeHLS**, a large-scale, open-source dataset for HLS DSE and QoR prediction. By aggregating diverse real-world and synthetic HLS C++ kernels, ForgeHLS surpasses existing datasets in scale, offering over 536 kernels and 429,276 designs, 10 times larger than prior datasets. Additionally, we developed an automated pragma insertion workflow, enabling direct pragma embedding into the source code to make generated HLS designs easier to use. Using this dataset, we conducted two representative downstream tasks: QoR prediction and HLS pragma insertion. These tasks demonstrate the utility of ForgeHLS in HLS optimization and highlight its potential for advancing research in the EDA area.



# REFERENCES

- [1] M. Gao, J. Zhao, Z. Lin, and M. Guo, "Hierarchical source-to-post-route qor prediction in high-level synthesis with gnns," in *DATE*, 2024.
- [2] N. Wu *et al.*, "High-level synthesis performance prediction using gnns: Benchmarking, modeling, and advancing," in *DAC*, 2022.
- [3] Z. Lin, Z. Yuan, J. Zhao, W. Zhang, H. Wang, and Y. Tian, "Powergear: Early-stage power estimation in fpga hls via heterogeneous edge-centric gnns," in *Procs. of Design, Automation and Test in Europe Conference and Exhibition (DATE)*, 2022.
- [4] Z. Lin, J. Zhao, S. Sinha, and W. Zhang, "Hl-pow: A learning-based power modeling framework for high-level synthesis," in *2020 25th Asia and South Pacific Design Automation Conference (ASP-DAC)*, 2020, pp. 574–580.
- [5] A. Sohrabizadeh, C. H. Yu, M. Gao, and J. Cong, "Autodse: Enabling software programmers to design efficient fpga accelerators," 2021. [Online]. Available: <https://arxiv.org/abs/2009.14381>
- [6] H. Kuang, X. Cao, J. Li, and L. Wang, "Hgbo-dse: Hierarchical gnn and bayesian optimization based hls design space exploration," in *2023 ICFPT*, 2023, pp. 106–114.
- [7] L. Ferretti, J. Kwon, G. Ansaloni, G. Di Guglielmo, L. Carloni, and L. Pozzi, "Db4hls: A database of high-level synthesis design space explorations," *IEEE Embedded Systems Letters*, vol. 13, no. 4, pp. 194–197, 2021.
- [8] S. Abi-Karam, R. Sarkar, A. Seigler, S. Lowe, Z. Wei, H. Chen, N. Rao, L. John, A. Arora, and C. Hao, "Hls-factory: A framework empowering high-level synthesis datasets for machine learning and beyond," in *Proceedings of the 2024 ACM/IEEE International Symposium on Machine Learning for CAD*, 2024, pp. 1–9.
- [9] Z. Wei, A. Arora, R. Li, and L. John, "Hlsdataset: Open-source dataset for ml-assisted fpga design using high level synthesis," in *2023 IEEE 34th International Conference on ASAP*. IEEE, 2023, pp. 197–204.
- [10] Y. Bai, A. Sohrabizadeh, Z. Qin, Z. Hu, Y. Sun, and J. Cong, "Towards a comprehensive benchmark for high-level synthesis targeted to fpgas," *Advances in Neural Information Processing Systems*, vol. 36, pp. 45 288–45 299, 2023.
- [11] "https://github.com/xilinx/vitis-hls-introductory-examples."
- [12] T. Yuki and Louis-Noël, "Pouchet. polybench/c."
- [13] Y. Hara, H. Tomiyama, S. Honda, H. Takada, and K. Ishii, "Chstone: A benchmark program suite for practical c-based high-level synthesis," in *2008 IEEE International Symposium on Circuits and Systems (ISCAS)*. IEEE, 2008, pp. 1192–1195.
- [14] B. Reagen, R. Adolf, Y. S. Shao, G.-Y. Wei, and D. Brooks, "Machsuite: Benchmarks for accelerator design and customized architectures," in *2014 IEEE IISWC*. IEEE, 2014, pp. 110–119.
- [15] Y. Zhou, U. Gupta, S. Dai, R. Zhao, N. Srivastava, H. Jin, J. Featherston, Y.-H. Lai, G. Liu, G. A. Velasquez *et al.*, "Rosetta: A realistic high-level synthesis benchmark suite for software programmable fpgas," in *Proceedings of the 2018 ACM/SIGDA International Symposium on Field-Programmable Gate Arrays*, 2018, pp. 269–278.
- [16] G. Zhong *et al.*, "Design space exploration of fpga-based accelerators with multi-level parallelism," in *DATE*, 2017, pp. 1141–1146.
- [17] S. Dai *et al.*, "Fast and accurate estimation of quality of results in high-level synthesis with machine learning," in *FCCM*, 2018.
- [18] A. Sohrabizadeh *et al.*, "Automated accelerator optimization aided by graph neural networks," in *DAC*, 2022.
- [19] J. Zhao, L. Feng, S. Sinha, W. Zhang, Y. Liang, and B. He, "Comba: A comprehensive model-based analysis framework for high level synthesis of real applications," in *ICCAD*. IEEE, 2017, pp. 430–437.
- [20] F. Ferrandi, P. L. Lanzi, D. Loiacono, C. Pilato, and D. Sciuto, "A multi-objective genetic algorithm for design space exploration in high-level synthesis," in *2008 IEEE Computer Society Annual Symposium on VLSI*. IEEE, 2008, pp. 417–422.
- [21] B. C. Schafer, T. Takenaka, and K. Wakabayashi, "Adaptive simulated annealer for high level synthesis design space exploration," in *2009 International Symposium on VLSI Design, Automation and Test*. IEEE, 2009, pp. 106–109.
- [22] N. Wu, Y. Xie, and C. Hao, "Ironman: Gnn-assisted design space exploration in high-level synthesis via reinforcement learning," in *Proceedings of the 2021 on Great Lakes Symposium on VLSI*. IEEE, 2021, pp. 39–44.
- [23] S. Pouget, L.-N. Pouchet, and J. Cong, "Automatic hardware pragma insertion in high-level synthesis: A non-linear programming approach," *arXiv preprint arXiv:2405.12304*, 2024, first article.
- [24] S. Pouget, L.-N. Pouchet, and J. Cong, "Enhancing high-level synthesis with automated pragma insertion and code transformation framework," *arXiv preprint arXiv:2405.03058*, 2024, second article.
- [25] Z. Li, C. Xu, Z. Shi, Z. Peng, Y. Liu, Y. Zhou, L. Zhou, C. Ma, J. Zhong, X. Wang, J. Zhao, Z. Chu, X. Yang, and Q. Xu, "Deepcircuitx: A comprehensive repository-level dataset for rtl code understanding, generation, and ppa analysis," 2025.
- [26] LeetCode, "Leetcode: The world's leading coding platform," 2025, accessed: 2025-04-17. [Online]. Available: <https://www.leetcode.com>
- [27] E. J. Hu, Y. Shen, P. Wallis, Z. Allen-Zhu, Y. Li, S. Wang, L. Wang, and W. Chen, "Lora: Low-rank adaptation of large language models," 2021.